Wearable Sensor System for Detecting Gait Parameters of Abnormal Gaits: A Feasibility Study

Guangyi Li, Tao Liu, *Senior Member, IEEE*, and Jingang Yi, *Senior Member, IEEE*

***Abstract*— The goal of this paper is to evaluate the feasibility of a wearable, low-cost optical, inertial, and force sensor suite for measuring the gait parameters of an abnormal gait. A pair of wearable shoes fused with range sensor arrays (WSFRSA) are developed for the gait analysis of normal and abnormal human walking. With the multiple small-size insole force sensors, the WSFRSA provides the real-time gait parameter estimations, such as normalized foot peak pressure, stance ratio, walking velocity, step-time variability, and so on. The fusion scheme is implemented to integrate the gyroscope and the range sensor measurements to obtain the foot pose estimation. We focus on the feasibility study and comparison of the gait parameters estimation using the WSFRSA and other methods. The results show a significantly less stride length and walking velocity, higher stance ratio, and step-time variability in the abnormal gait without toe rotation than those in normal walking gait. The WSFRSA shows highly agreement results with the reference system and acceptable performance for detecting the abnormal gait without the toe rotation.**

***Index Terms*— Gait parameters, sensor fusion, human walking gaits, extended Kalman filter, wearable sensors.**

I. Introduction

DIABETES mellitus, a chronic disease caused by the body's inability to produce or use insulin, can result in other body disorders such as a high risk of fall [1] and the forefoot ulcers [2]. Gait characteristics of diabetic patients are important for clinical researchers and practitioners to assess patients' health conditions. Optical motion capture systems (e.g., [3]) are widely used in laboratory environment as a standard tool for gait analysis. Stationary force plates are also used to provide the ground reaction force (GRF) measurements to estimate the joint torques/forces. However, these tools and devices are impracticable for gait analysis of personal daily living or outdoor activities.

Various wearable sensors are developed for ambulatory gait assessment. For example, a single accelerometer is used to measure the trunk's acceleration to provide motion spatiotemporal parameters [4], [5]. Similarly, a single gyroscope is proposed to detect the angular velocity of one thigh in the sagittal plane for calculating stride length and walking velocity [6]. Although it is light, low-cost, convenient and nonintrusive to human movement, the gait estimation results by single gyroscope or accelerometer are not accurate. Therefore, multiple wearable sensors are needed to obtain the accurate gait movements (e.g., [7]). Integrated accelerometers and gyroscopes devices such as inertial measurement unit (IMU) are also commonly used in gait estimation [8]–[10]. In [11], a set of accelerometers are placed on most human segments to obtain highly accurate measurements but this can bring inconvenience and intrusive influence on ambulatory movements. In [12]–[14], single- or double-pendulum models are employed to reduce the number of wearable sensors and to extract gait characteristics.

Wearable insole sensors can obtain the foot pressure or pressure distribution to predict gait parameters or detect gait events [15], [16]. The insoles are thin, flexible, easy installation, and noninstrusive for human gait [16]–[18]. Other low-cost systems, such as laser range scanner [19] or cheap cameras, are not available for use in daily living activities. In [20] and [21], IMU and range sensors are integrated together to build a sensor fusion-based gait analysis. The positions of the IMU are obtained by double-integration of the accelerometer measurements and the results might not be reliable even under fusion treatments, such as zero position or velocity resets with gait events. In [22], several infra-red (IR) sensors are mounted on high-heeled shoes with restrictive toe joint movement in the sagittal plane. The calculation in [22] neglects the influence of the roll angle on the sensor measurements, which can result in significant errors in abnormal gaits. Moreover, the subjects' gaits were likely influenced because of the use of high-heeled shoes in experiments. As pointed out in [23], some gait parameters are different between walking with shoes and those under barefoot.

In this paper, we present a development of a pair of wearable shoes fused with range sensor arrays (WSFRSA). The WSFRSA is built on our previous work in [24]–[26]. Both kinetic and kinematic measurements are obtained by the WSFRSA and the wearing comfort is guaranteed by the small size and relatively light weight of the smart shoes. The main goal of this paper is to present the feasibility of assessing gait parameters using the WSFRSA. Gait parameters are key indicators for evaluating the abnormalities [27]. These parameters are also widely used in many other applications, for example, variability in different walking conditions [28] and in transtibial amputee falls [29], classification of neurological disorders [30], assessment of older adults [31], and biomechanical modifications in diabetic foot

Manuscript received January 20, 2018; accepted January 26, 2018. Date of publication March 12, 2018; date of current version April 23, 2018. This work was supported in part by the NSFC under Grant 51775485 and Grant U1613203, in part by the Zhejiang Provincial Natural Science Foundation of China under Grant LR15E050002, in part by the State Key Laboratory of Fluid Power and Mechatronic Systems under Grant GZKF-201702, and in part by the Fundamental Research Funds for the Central Universities under Grant 2018QNA4004. The associate editor coordinating the review of this paper and approving it for publication was Dr. Jürgen Kosel. *(Corresponding author: Tao Liu.)*

G. Li and T. Liu are with The State Key Laboratory of Fluid Power and Mechatronic Systems, School of Mechanical Engineering, Zhejiang University, Hangzhou 310027, China (e-mail: li_guangyi@zju.edu.cn; liutao@zju.edu.cn).

J. Yi is with the Department of Mechanical and Aerospace Engineering, Rutgers University, Piscataway, NJ 08854 USA (e-mail: jgyi@rutgers.edu).

Digital Object Identifier 10.1109/JSEN.2018.2814994

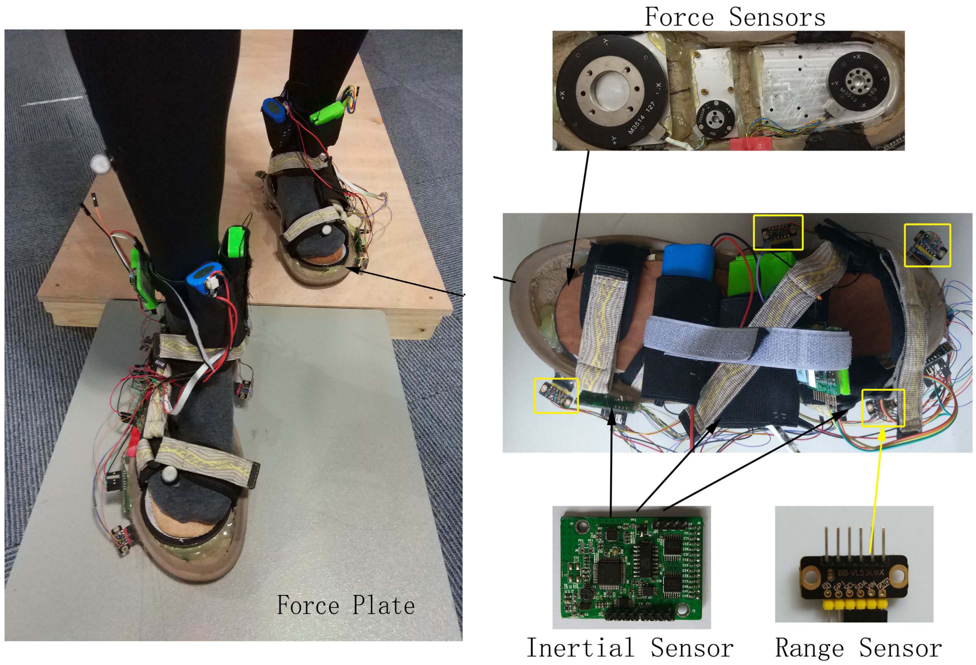

Fig. 1. The wearable shoe sensor suit (force sensors, inertial sensors and range sensors).

patients [2], etc. The main contribution of the work primarily lies in the wearable systems development of the small-size, light-weight force sensors with the IR range sensors for walking gait parameter estimation. The foot pose estimation method is simple to implement and avoids the integration of acceleration measurements. We validate and demonstrate the feasibility of the WSFRSA for gait parameter estimation for normal and abnormal gaits.

II. Materials and Methods

A. Wearable Shoes Fused With Range Sensor Arrays

Built on the sensor shoes in the wearable gait analysis system (WGAS) [24], [25], the WSFRSA is developed with a pair of smart shoes with four range sensors (VL53L0x, STM, Switzerland) on the edge of each shoe. As shown in Fig. 1, the wearable shoes contain six force sensors at the heel, arch and forefoot locations. The force sensors circuits are integrated with inertial sensors (MPU9250, InvenSense, USA) and mounted nearby the corresponding force sensors. Unlike the WGAS, the attitudes of the force sensors under the arch can be obtained. For each shoe, three range sensors are mounted around the heel force sensor and the fourth range sensor is mounted on the location of the forefoot. For each shoe, a WiFi module is used to send the measurements of the force sensors and the inertial sensors to a nearby personal computer. A small circuit (Bluno Nano, DFRobot) is used to sample the measurements of the four range sensors and transmit the collected data to the personal computer via another WiFi module.

B. Fusion Method

The fusion method is implemented in an extended Kalman filter (EKF) scheme. In the following, we present the EKF scheme into steps: EKF prediction of the state vector, measurements and observation calculation, and EKF update with correction. A similar EKF implementation can be found in [32] and [33].

1) EKF State Vector Prediction: Fig. 1 illustrates the layout of the force sensor, IMU, and range sensors mounted on the shoes. The global coordinate system for navigation is defined as the x-axial positive direction points to the east, the y-axial positive direction points to the north, and the z-axial positive direction is upright. The IMU attitude is represented by quaternion $\boldsymbol{q}$. The kinematic relationship of $\boldsymbol{q}$ in the body frame is expressed as [34].

$$\boldsymbol{q}_k^- = \boldsymbol{\Phi}_k \boldsymbol{q}_{k-1}, \tag{1}$$

where $\boldsymbol{q}_k^-$ denotes the quaternion prediction of the kth step, $k \in \mathbb{N}$. The coefficient matrix $\boldsymbol{\Phi}_k$ in (1) is given as

$$\boldsymbol{\Phi}_k = \begin{bmatrix} 1 & -\frac{1}{2}\omega_k^x T & -\frac{1}{2}\omega_k^y T & -\frac{1}{2}\omega_k^z T \\ \frac{1}{2}\omega_k^z T & 1 & \frac{1}{2}\omega_k^y T & -\frac{1}{2}\omega_k^z \\ \frac{1}{2}\omega_k^y T & -\frac{1}{2}\omega_k^z T & 1 & \frac{1}{2}\omega_k^x T \\ \frac{1}{2}\omega_k^z T & \frac{1}{2}\omega_k^y T & -\frac{1}{2}\omega_k^x T & 1 \end{bmatrix} \tag{2}$$

where $\boldsymbol{\omega}_k = \left[\omega_k^x \ \omega_k^y \ \omega_k^z\right]^T$ denotes the angular velocity measurements by the gyroscope at the kth step, and T is the sampling period.

2) EKF Measurements and Outputs: We assume that the range sensors are all mounted on the same XOY plane along the shoe sole with the IMU and force sensor. A local frame XYZ is setup along with the IMU. For the ith range sensor, the distance measurement is denoted as d_i and its height is denoted by h_i, $i = 1, 2, 3$. We also denote the pitch, roll and yaw angles of the shoe sole (same for IMU) as θ, φ and ψ, respectively. It is straightforward to obtain

$$h_i = d_i \cos\theta \cos\varphi. \tag{3}$$

We also define $\boldsymbol{d}_i = [0\ 0\ d_i]^T$, $i = 1, 2, 3$, are the space vectors of measuring paths in the positive direction of the local coordinate system. From (3), three range sensors are sufficient to calculate the pitch and roll angles, that is, θ and φ, but not for yaw angle ψ.

To obtain the calculation of θ and φ, we denote the position of the ith range sensor as S_i, $i = 1, 2, 3$. Along line $\overline{S_1S_2}$, a point S_4 is chosen such that line $\overline{S_3S_4}$ is perpendicular to $\overline{S_1S_2}$. From measured distances d_1 and d_2, we calculate

$$d_4 = d_1 + \frac{l_{14}}{l_{12}}(d_2 - d_1), \tag{4}$$

where l_{14} and l_{12} denote the lengths of line segments $\overline{S_1S_4}$ and $\overline{S_1S_2}$, respectively. The calculations of θ and φ are given as

$$\theta = \tan^{-1}\left(\frac{d_4 - d_3}{l_{34}}\right), \quad \varphi = \tan^{-1}\left(\frac{(d_2 - d_1)\cos\theta}{l_{12}}\right), \tag{5}$$

where l_{34} is the length of line segment $\overline{S_3S_4}$.

Let $\boldsymbol{p}_i$ denote the relative position vector from the ith range sensor to the IMU in the local frame, $i = 1, 2, 3$, and $\boldsymbol{p}^n$ denote the IMU position vector in the global frame. From the geometric relationship, we obtain

$$\boldsymbol{e}_3\boldsymbol{p}^n = \boldsymbol{e}_3\boldsymbol{C}^{bn}\left(\boldsymbol{d}_i + \boldsymbol{p}_i\right), \quad i = 1, 2, 3, \tag{6}$$

where $\boldsymbol{e}_3 = [0\ 0\ 1]^T$ and matrix $\boldsymbol{C}^{bn}$ represents the rotation matrix from the local to the global frames. Since it is difficult to accurately obtain the IMU position (i.e., $\boldsymbol{p}^n$), we consider the observations of range sensor heights

$$h_i = \boldsymbol{e}_3\boldsymbol{C}^{bn}\boldsymbol{d}_i, \quad i = 1, 2, 3. \tag{7}$$

Let $\boldsymbol{d}_{ij} = \boldsymbol{d}_j - \boldsymbol{d}_i$ denote the relative position vectors between the ith and jth range sensors in the local frame, $i, j = 1, 2, 3$, $i \neq j$. Since the range sensors heights in the global frame are acquired directly, another set of observations are taken as the their differences, that is,

$$h_{ij} := h_j - h_i = \boldsymbol{e}_3\boldsymbol{C}^{bn}\boldsymbol{d}_{ij}, \quad i, j = 1, 2, 3,\ i \neq j. \tag{8}$$

If we consider the force sensor frame and all vectors $\boldsymbol{d}_i$ are represented in the WSFRSA frame, the observation equations (7) and (8) are then modified as

$$h_i = \boldsymbol{e}_3\boldsymbol{C}^{bn}\boldsymbol{C}^{fb}\boldsymbol{d}_i, \quad h_{ij} = \boldsymbol{e}_3\boldsymbol{C}^{bn}\boldsymbol{C}^{fb}\boldsymbol{d}_{ij}, \tag{9}$$

for $i, j = 1, 2, 3$, $i \neq j$, where matrix $\boldsymbol{C}^{fb}$ represents the rotation matrix from the force sensor frame to the IMU local frame. In summary, the measurements and observation of the EKF implementation are defined as

$$\boldsymbol{z} = \begin{bmatrix} h_1 & h_2 & h_3 & h_{12} & h_{23} & h_{31} \end{bmatrix}^T. \tag{10}$$

Before updating vector $\boldsymbol{z}$, the normalized innovations squared (NIS) method [20] is calculated and if the NIS exceeds a threshold value, the update of vector $\boldsymbol{z}$ is rejected.

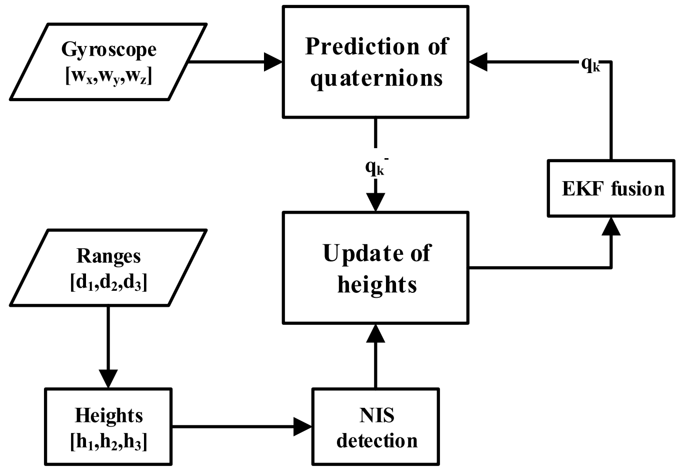

Fig. 2. The structure of the fusion method.

3) State Vector Update With Measurements: The state vector (i.e., quaternion $\boldsymbol{q}$) is updated by using the measurements and observation vector $\boldsymbol{z}$ at the kth step as

$$\boldsymbol{q}_k = \boldsymbol{q}_k^- + \boldsymbol{K}_k\left(z_k - \boldsymbol{H}_k\boldsymbol{q}_k^-\right), \tag{11}$$

where Jacobian matrix $\boldsymbol{H}_k$ of the measurements and observation is calculated as $\boldsymbol{H}_k = \left.\frac{\partial z}{\partial \boldsymbol{q}}\right|_{\boldsymbol{q}_k^-}$. The EKF gain $\boldsymbol{K}_k$ is updated as is:

$$\boldsymbol{K}_k = \boldsymbol{P}_k^-\boldsymbol{H}_k^T(\boldsymbol{H}_k\boldsymbol{P}_k^-\boldsymbol{H}_k^T + \boldsymbol{R})^{-1}, \quad \boldsymbol{P}_k^- = \boldsymbol{\Phi}_k\boldsymbol{P}_{k-1}\boldsymbol{\Phi}_k^T + \boldsymbol{Q},$$

where $\boldsymbol{R}$ and $\boldsymbol{Q}$ denote the measurement noise and state dynamics covariance matrices, respectively. The state error covariance matrix $\boldsymbol{P}$ is updated as

$$\boldsymbol{P}_k = (\boldsymbol{I} - \boldsymbol{K}_k\boldsymbol{H}_k)\boldsymbol{P}_k^-.$$

C. Extraction Method of Gait Characteristics

Reliable gait parameters includes normalized peak pressure, walking velocity, stride length, stance ratio, and step-time variability and we briefly discuss here.

1) Normalized Peak Pressure: The normalized peak pressure is the ratio of the peak value of the GRF in the vertical direction and the subject's body weight. Two peak pressures commonly appear in the GRF profile during each stance: one after the heel-strike event and the other before the toe-off event. The peak pressure values are obtained from the GRF data by the force sensors.

2) Stance Ratio: We use the GRF measurements to determine the gait events such as heel-strike and toe-off. For one leg, the time duration of the two adjacent heel-strike events is defined as the cycle time. The cycle time is divided into stance time and swing time by the toe-off event. The stance ratio is defined as the ratio of the stance time and the cycle time.

3) Step-Time Variability: Step time is defined as the duration between two adjacent heel-strike events. The standard deviation (SD) of step time is used as its variability.

4) Stride Length: Stride length can be computed by various approaches, such as integration of linear acceleration, a velocity compensation [10], [35]. This method is applied in the WSFRSA. The step length L can be also estimated by using a simplified double-pendulum model for lower limbs motion [12]. Using this method with the WGAS system, we obtain

$$L = l_{sh}\sin(\alpha_1+\alpha_3)+l_{th}\sin\alpha_1+l_{th}\sin\alpha_2+l_{sh}\sin(\alpha_2-\alpha_4),$$

where angles α_1 (α_2) is the extension (flexion) angle of the hip of the posterior (anterior) leg, α_3 (α_4) is the flexion angle of the knee of the posterior (anterior) leg, l_{sh} and l_{th} are the lengths of the shank and the thigh, respectively. The stride length is the sum of the two nearby step lengths.

5) Walking Velocity: The walking velocity is estimated by dividing the stride length by the cycle time.

III. Experimental Methods

An optical motion capture system (from Vicon Inc.) and a stationary force plate (model BP400600-2000 from AMTI Inc.) are used to provide the ground truth for gait and force measurements for evaluation purpose. The motion capture systems are synchronized with the force plate through a wired trigger signal. Eight male subjects (age: 22 to 25 years old, weight: 50 to 86 kg, height: 170 to 178 cm) were recruited in the experiment. These subjects were reported without disability or history of injury on their lower extremities. The subjects were informed the procedure of the research in accordance with the Declaration of Helsinki, and the protocol was approved by the Medical Ethics Committee of School of Medicine, Zhejiang University.

A. Validation of the Fusion Method

To validate the fusion method, four subjects were asked to wear the WSFRSA to walk in an indoor laboratory. Due to confined space (about 4 meters long), the subjects walked for about 5 to 6 steps with normal walking speed. Three optical markers were attached at the positions of the three range sensors around the heel of each shoe to provide the ground truth attitude information for IMU [36]. Each subject conducted 15 trails in the experiments.

B. Validation of the Gait Parameters

To validate the gait parameter estimation, the rest four subjects were asked to wear the WSFRSA to conduct the experiments. Sixteen optical markers were placed on anatomical landmarks (anterior superior iliac spines, posterior superior iliac spines, knee joints, thighs, shanks, ankle joints, toes, heels) of lower extremities. After calibration, the subjects walked in an indoor laboratory with their right feet standing on the force plate. Each subject conducted both the normal and abnormal walking gaits and each repeated 30 trials. The abnormal gait was generated by restrain the rotation of the toe joint in walking. The shoe sole were fixed on a wooden board in the controlled abnormal gait trials such that the subjects' toe joints cannot rotate during walking. Before each trial, a five-minute break was taken to prevent any fatigue effect. The positions of the IMU and range sensors on the shoe sole were also checked to guarantee the consistence in all experiments. The gait parameters were calculated off-line using Matlab software package (from the Mathworks Inc., USA). The temporal parameters of the reference system were calculated by additionally utilizing the z-axis positions of the markers on the heels. The gait events (e.g., heel-strike and toe-off) were detected by comparing the z-axial position with the a threshold value.

To compare the performance differences between the WSFRSA and the WGAS, all eight subjects were asked to wear the WGAS with sixteen optical markers similar to the above described experiments. Each subject conducted and repeated 12 trails in normal walking experiments.

TABLE I

Comparison Results Between the Heights Calculated by the Range Sensors' Measurements and the Ground Truth

	Range Sensors		
	1	2	3
R	0.986	0.980	0.974
RMSE	13.34	10.97	10.30

IV. Results

A. Validation Results of the Fusion Method

Table I shows the comparison results of the range sensors and the ground truth. Three markers z-axis positions were considered as the reference values. Root mean square error (RMSE) and correlation coefficient (R) are employed to illustrate the comparison results. Fig. 3 shows a sample of height comparison between the range sensors and marker-based measurements. These samples were chosen randomly from the measurements. Table II shows the comparison results of the attitude angles between the EKF fusion method and the reference system. For comparison purpose, the results obtained by using the motion processor library algorithm (MPL) is also included in Table II. Fig. 4 shows the comparison profiles of three randomly-selected samples. These plots includes the results by the EKF fusion (blue dash lines), the 9-axis fusion method provided by MPL (green dot dash lines), and the ground truth (red solid lines). From all results shown in these tables and figures, the EKF fusion approach with the range sensor implementation closely matches the ground truth and also demonstrates superior performance comparing with the MPL method.

B. Gait Parameters

Table III shows the normal gait parameters calculated by the measurements of the WSFRSA and the reference system. Table IV shows the gait parameters results of the abnormal gait by the WSFRSA system. Table V shows the normal gait parameters calculated by the measurements of the WGAS and the reference system. The results of normalized peak pressure, stance ratio, walking velocity, and stride length are expressed

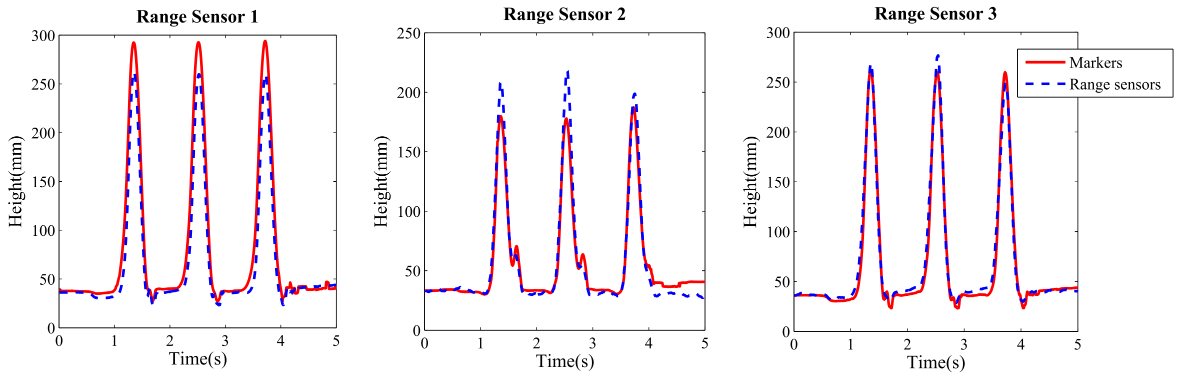

Fig. 3. Comparison results between the heights calculated by the range sensors' measurements and the z-axis positions of the markers.

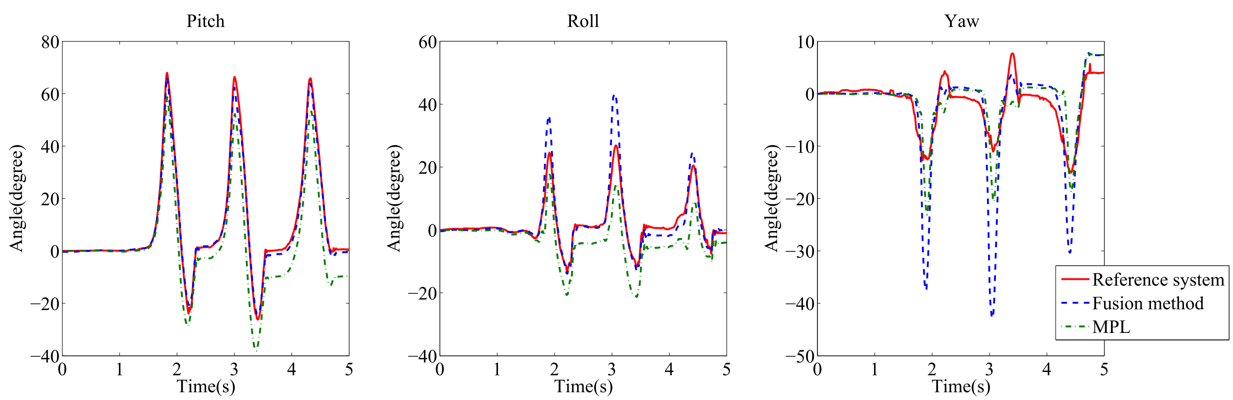

Fig. 4. Comparison results between the attitude angles calculated by the fusion method and the reference system.

TABLE II
COMPARISON RESULTS BETWEEN THE ATTITUDE ANGLES CALCULATED BY THE FUSION METHOD AND THE REFERENCE SYSTEM

		Attitude Angles		
		Pitch	**Roll**	**Yaw**
R	**Fusion**	0.994	0.935	0.795
	MPL	0.957	0.813	0.673
RMSE	**Fusion**	2.84	4.75	6.75
	MPL	9.83	6.11	4.98

as the mean value with their standard deviations (SD) from multiple subjects and trails. The step-time variability results are expressed as their mean values. The comparison between the reference systems and the WSFRSA and WGAS is expressed as the average percentage error. Fig. 5 shows the statistical results (i.e., histogram) of the gait parameters in both the normal and abnormal walking experiments.

V. DISCUSSIONS

We mainly use the experiments of healthy subjects to demonstrate the feasibility of using the WSFRSA to detect the gait parameters of abnormal gait. To achieve the goal, measurements of wearable IMU are fused with the three range sensors on the shoe sole. Other fusion method such as integration of magnetic sensors with inertial sensors is vulnerable to environmental or motion disturbances. Our approach instead uses the optical range sensors for foot pose estimation. The experimental validation of our fusion method demonstrates high agreement in the foot clearance estimation with the optical motion capture system. For instance, three range sensors' height estimates show high correlation coefficients and RMSEs, i.e., 0.986, 0.980, and 0.974, and 13.34 mm, 10.97 mm, and 10.30 mm, respectively, with the ground truth.

From Fig. 3, it becomes clear that the relatively large errors occur at the moments around the peak values of the heel height. This is primarily due to the use of the range sensors. The heel's inclined angle and the ankle plantar-flexion angle almost reaches their maximum values simultaneously and the range sensor accuracy deteriorates at these moments because of the large inclined angles between the range sensors and the ground.

In experiments, the sampling frequency of the range sensor measurements is about 33 Hz and the height estimates are not accurate under fast foot movement. The correlation coefficients and the RMSE results in Table II show that the EKF fusion generates superior attitude estimation than that of the MPL method. The EKF fusion particularly shows excellent agreement of the pitch angle estimation to the ground truth. Moreover, as also shown in Fig. 4, the estimation results of the yaw angle are worse than those of the pitch and roll angles. This is not surprising because the range sensor measurements are insensitive to the yaw angle during walking gaits. In [20], only one ultrasound sensor is used to measure the relative position of the foot and the measurement is not successive. In [20] and [21], the accuracy of the fusion

TABLE III
GAIT PARAMETERS OF NORMAL GAIT CALCULATED BY THE MEASUREMENTS OF THE WSFRSA AND THE REFERENCE SYSTEM

Gait Parameters	Reference System	WSFRSA	Percentage error(%)
Normalized peak pressure(N/kg)	10.64 ± 0.19	10.69 ± 0.50	4.23
Stance ratio(%)	59.19 ± 2.32	59.78 ± 3.08	5.20
Stride length(m)	0.98 ± 0.08	1.02 ± 0.09	9.34
Velocity(m/s)	0.93 ± 0.07	0.94 ± 0.10	5.90
Step-time variability(ms)	45	44	2.23

TABLE IV
GAIT PARAMETERS OF THE ABNORMAL GAIT WITH RESTRICTION OF TOE JOINT CALCULATED BY THE MEASUREMENTS OF THE WSFRSA AND THE REFERENCE SYSTEM

Gait Parameters	Reference System	WSFRSA	Percentage error(%)
Normalized peak pressure (N/kg)	10.09 ± 0.23	10.34 ± 0.31	4.17
Stance ratio (%)	66.67 ± 5.19	68.55 ± 4.78	7.26
Stride length (m)	0.88 ± 0.12	0.86 ± 0.12	9.48
Walking velocity (m/s)	0.80 ± 0.07	0.82 ± 0.11	9.92
Step-time variability (ms)	88	94	7.44

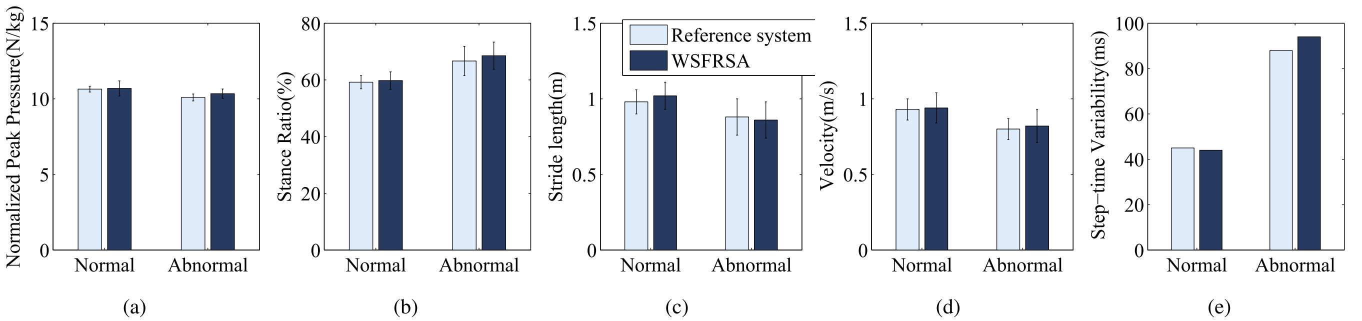

Fig. 5. Comparison results between the WSFRSA and the reference system in normal gait and the abnormal gait without toe rotation effects. (a) Normalized peak pressure; (b) Stance ratio; (c) Stride length; (d) Velocity; (e) Step-time variability.

TABLE V
GAIT PARAMETERS OF NORMAL GAIT CALCULATED BY THE MEASUREMENTS OF THE WGAS AND THE REFERENCE SYSTEM

Gait Parameters	Reference System	WGAS	Percentage error(%)
Normalized peak pressure(N/kg)	10.39 ± 0.16	10.64 ± 0.97	5.6
Stance ratio(%)	60.95 ± 1.13	62.26 ± 2.86	4.2
Stride length(m)	1.32 ± 0.05	1.09 ± 0.08	17.6
Velocity(m/s)	1.47 ± 0.12	1.25 ± 0.14	14.7
Step-time variability(ms)	54	111	135.3

methods depends on the IMU positions, which are obtained by double integration of the accelerometer measurements and therefore, are not accurate due to drifting noises.

The results in Tables III and IV confirm that the WSFRSA calculates the gait parameters closely with the ground truth for both the normal and abnormal walking gaits. From the comparison results shown in Fig. 5, we clearly see that the abnormal gait parameters show significantly different values from these under the normal gait. Without toe rotation, the normalized peak pressure decreases significantly since it is difficult to decelerate or accelerate at the heel-strike and toe-off events. This also results in a larger value of the stance ratio than that of normal gait. The step-time variability of the abnormal gait significantly increases compared to the normal gait and this could be related to an increased demand on balance control without toe rotation. The stride length and the walking velocity under the abnormal gait are smaller than these under the normal gait. The subjects need additional time to keep balance and the motion of foot slows down to adapt to the GRF changes.

We also list and compare the performance of the WGAS for the normal gait experiments in Table V. For the gait parameters such as the normalized peak pressure and the stance ratio, the WGAS and the WSFRSA perform similarly and the calculations are close to the ground truth, that is, within around 5% relative errors. However, for the gait parameters such as stride length, walking velocity, and step-time variability, the calculation results by the WGAS are much worse than those by the WSFRSA. For example, the mean step-time variability by the WGAS is 111 ms, while the ground truth is around 54 ms. The large discrepancy of the WGAS calculation with the ground truth is mainly caused by the inaccurate gait events detection (i.e., heel-strike and toe-off) with the WGAS. These gait events are detected by using the force sensor measurements. The force measurements are not accurate when the foot-ground contact area is small, such as at the moments of heel-strike or toe-off. Because of using the force measurements, the stride length and velocity calculations also have large errors.

VI. Conclusion

In this paper, a pair of wearable shoes fused with range sensor arrays (WSFRSA) were developed for gait detection for normal gait and the abnormal gait without toe rotation. The range sensors were attached on the shoe soles to extract the height information. A sensing fusion design was developed to integrate the range sensor with the gyroscope measurements for foot pose estimation. We conduct multi-subject experiments to validate the fusion design performance. The experiments demonstrated high accuracy of the foot pitch and roll angles estimation with the ground truth for normal gait. Moreover, the gait parameter estimation by the WSFRSA showed highly agreements with the ground truth. We also conducted comparison experiments with the previously developed wearable gait analysis system (WGAS). The comparison results showed that the WSFRSA outperformed the WGAS in several gait parameters estimation such as the stride length, walking velocity, and the step-time variability, etc.

References

[1] L. Allet, S. Armand, A. Golay, D. Monnin, R. A. de Bie, and E. D. de Bruin, "Gait characteristics of diabetic patients: A systematic review," *Diabetes Metab Res. Rev.*, vol. 24, no. 3, pp. 173–191, 2008.

[2] G. Lamola *et al.*, "Quantitative assessment of early biomechanical modifications in diabetic foot patients: The role of foot kinematics and step width," *J. Neuroeng. Rehabil.*, vol. 12, no. 1, p. 98, 2015.

[3] *Vicon Vantage Helps Derby University Search for the Perfect Golf Swing*. Accessed: Dec. 2, 2015. [Online]. Available: https://www.vicon.com/press/2015-12-02/vicon-vantage-helps-derby-university-search-for-the-perfect-golf-swing

[4] W. Zijlstra and A. L. Hof, "Assessment of spatio-temporal gait parameters from trunk accelerations during human walking," *Gait Posture*, vol. 18, no. 2, pp. 1–10, Oct. 2003.

[5] F. Bugané *et al.*, "Estimation of spatial-temporal gait parameters in level walking based on a single accelerometer: Validation on normal subjects by standard gait analysis," *Comput. Methods Programs Biomed.*, vol. 108, no. 1, pp. 129–137, 2012.

[6] S. Miyazaki, "Long-term unrestrained measurement of stride length and walking velocity utilizing a piezoelectric gyroscope," *IEEE Trans. Biomed. Eng.*, vol. 44, no. 8, pp. 753–759, Aug. 1997.

[7] I. H. López-Nava *et al.*, "Estimation of temporal gait parameters using Bayesian models on acceleration signals," *Comput. Methods Biomech. Biomed. Eng.*, vol. 19, no. 4, p. 396, 2016.

[8] D. Novak, M. Goršič, J. Podobnik, and M. Munih, "Toward real-time automated detection of turns during gait using wearable inertial measurement units," *Sensors*, vol. 14, no. 10, p. 18800, 2014.

[9] J. Taborri, S. Rossi, E. Palermo, F. Patanè, and P. Cappa, "A novel HMM distributed classifier for the detection of gait phases by means of a wearable inertial sensor network," *Sensors*, vol. 14, no. 9, p. 16212, 2014.

[10] Q. Li, M. Young, V. Naing, and J. M. Donelan, "Walking speed estimation using a shank-mounted inertial measurement unit," *J. Biomech.*, vol. 43, no. 8, p. 1640, 2010.

[11] J. Petrofsky, S. Lee, and S. Bweir, "Gait characteristics in people with type 2 diabetes mellitus," *Eur. J. Appl. Physiol.*, vol. 93, nos. 5–6, pp. 640–647, 2005.

[12] A. Salarian, P. R. Burkhard, F. J. G. Vingerhoets, B. M. Jolles, and K. Aminian, "A novel approach to reducing number of sensing units for wearable gait analysis systems," *IEEE Trans. Biomed. Eng.*, vol. 60, no. 1, pp. 72–77, Jan. 2013.

[13] A. Salarian *et al.*, "Gait assessment in Parkinson's disease: Toward an ambulatory system for long-term monitoring," *IEEE Trans. Biomed. Eng.*, vol. 51, no. 8, pp. 1434–1443, Aug. 2004.

[14] K. Aminian, B. Najafi, C. Büla, P. F. Leyvraz, and P. Robert, "Spatio-temporal parameters of gait measured by an ambulatory system using miniature gyroscopes," *J. Biomech.*, vol. 35, no. 5, pp. 689–699, 2002.

[15] W. L. Hsi, H. M. Chai, and J. S. Lai, "Comparison of pressure and time parameters in evaluating diabetic footwear," *Amer. J. Phys. Med. Rehabil.*, vol. 81, no. 11, p. 822, 2002.

[16] F. Martínez-Martí *et al.*, "Embedded sensor insole for wireless measurement of gait parameters," *Austral. Phys. Eng. Sci. Med.*, vol. 37, no. 1, p. 25, 2014.

[17] M. Muñoz-Organero, C. Littlewood, J. Parker, L. Powell, C. Grindell, and S. Mawson, "Identification of walking strategies of people with osteoarthritis of the knee using insole pressure sensors," *IEEE Sensors J.*, vol. 17, no. 12, pp. 3909–3920, Dec. 2017.

[18] M. Muñoz-Organero, J. Parker, L. Powell, R. Davies, and S. Mawson, "Sensor optimization in smart insoles for post-stroke gait asymmetries using total variation and ℓ_1 distances," *IEEE Sensors J.*, vol. 17, no. 10, pp. 3142–3151, Dec. 2017.

[19] S. Tanabe *et al.*, "Spatiotemporal treadmill gait measurements using a laser range scanner: Feasibility study of the healthy young adults," *Physiol. Meas.*, vol. 38, no. 4, p. N81, 2017.

[20] D. Weenk, D. Roetenberg, B. J. van Beijnum, H. J. Hermens, and P. H. Veltink, "Ambulatory estimation of relative foot positions by fusing ultrasound and inertial sensor data," *IEEE Trans. Neural Syst. Rehabil. Eng.*, vol. 23, no. 5, pp. 817–826, May 2015.

[21] P. D. Duong and Y. S. Suh, "Foot pose estimation using an inertial sensor unit and two distance sensors," *Sensors*, vol. 15, no. 7, pp. 15888–15902, 2015.

[22] A. Arami, N. S. Raymond, and K. Aminian, "An accurate wearable foot clearance estimation system: Towards a real time measurement system," *IEEE Sensors J.*, vol. 17, no. 8, pp. 2542–2549, Aug. 2017.

[23] M. Elboim-Gabyzon and S. Rotchild, "Spatial and temporal gait characteristics of elderly individuals during backward and forward walking with shoes and barefoot," *Gait Posture*, vol. 52, pp. 363–366, Feb. 2016.

[24] G. Li, T. Liu, J. Yi, H. Wang, J. Li, and Y. Inoue, "The lower limbs kinematics analysis by wearable sensor shoes," *IEEE Sensors J.*, vol. 16, no. 8, pp. 2627–2638, Aug. 2016.

[25] G. Li, T. Liu, L. Gu, Y. Inoue, H. Ning, and M. Han, "Wearable gait analysis system for ambulatory measurement of kinematics and kinetics," in *Proc. IEEE Sensors*, Valencia, Spain, Nov. 2014, pp. 1316–1319.

[26] M. Trkov, J. Yi, T. Liu, and K. Li, "Shoe-floor interactions human walking with slips: Modeling and experiments," *ASME J. Biomech. Eng.*, vol. 140, no. 3, pp. 031005-1–031005-11, 2018.

[27] V. Macellari, C. Giacomozzi, and R. Saggini, "Spatial-temporal parameters of gait: Reference data and a statistical method for normality assessment," *Gait Posture*, vol. 10, no. 2, p. 171, 1999.

[28] J. H. Hollman, M. K. Watkins, A. C. Imhoff, C. E. Braun, K. A. Akervik, and D. K. Ness, "A comparison of variability in spatiotemporal gait parameters between treadmill and overground walking conditions," *Gait Posture*, vol. 43, pp. 204–209, Jan. 2016.

[29] B. G. Hordacre, C. Barr, B. L. Patritti, and M. Crotty, "Assessing gait variability in transtibial amputee fallers based on spatial-temporal gait parameters normalized for walking speed," *Arch. Phys. Med. Rehabil.*, vol. 96, no. 6, p. 1162, 2015.

[30] C. Pradhan *et al.*, "Automated classification of neurological disorders of gait using spatio-temporal gait parameters," *J. Electromyography Kinesiol.*, vol. 25, no. 2, pp. 413–422, 2015.

[31] J. H. Hollman, E. M. Mcdade, and R. C. Petersen, "Normative spatiotemporal gait parameters in older adults," *Gait Posture*, vol. 34, no. 1, p. 111, 2011.

[32] J. Yi, H. Wang, J. Zhang, D. Song, S. Jayasuriya, and J. Liu, "Kinematic modeling and analysis of skid-steered mobile robots with applications to low-cost inertial measurement unit-based motion estimation," *IEEE Trans. Robot.*, vol. 25, no. 5, pp. 1087–1097, May 2009.

[33] Y. Zhang, K. Chen, and J. Yi, "Rider trunk and bicycle pose estimation with fusion of force/inertial sensors," *IEEE Trans. Biomed. Eng.*, vol. 60, no. 9, pp. 2541–2551, Sep. 2013.

[34] E. Brookner, *Tracking and Kalman Filtering Made Easy*. Hoboken, NJ, USA: Wiley, 1998.

[35] Y. L. Hsu, J. S. Wang, and C. W. Chang, "A wearable inertial pedestrian navigation system with quaternion-based extended kalman filter for pedestrian localization," *IEEE Sensors J.*, vol. 17, no. 10, pp. 3193–3206, May 2017.

[36] G. S. Faber, C. C. Chang, P. Rizun, and J. T. Dennerlein, "A novel method for assessing the 3-D orientation accuracy of inertial/magnetic sensors," *J. Biomech.*, vol. 46, no. 15, pp. 2745–2751, 2013.

Guangyi Li received the B.S. degree in electronic science and technology from the Huazhong University of Science and Technology, China, in 2013. He is currently pursuing the Ph.D. degree in mechatronic engineering with Zhejiang University, Hangzhou. His current research interests include wearable sensor system for gait analysis, robot vision in force measuring, and machine learning with application to signal processing and identification.

Tao Liu (M'08–SM'15) received the B.S. degree in mechanical engineering from the Harbin University of Science and Technology, Harbin, China, in 2001, the M.Eng. degree in mechanical engineering from the Harbin Institute of Technology, Harbin, in 2003, and the Ph.D. degree in engineering from the Kochi University of Technology, Kochi, Japan, in 2006. From 2009 to 2013, he was an Assistant Professor with the Department of Intelligent Mechanical Systems Engineering, Kochi University of Technology. He is currently a Professor with the State Key Laboratory of Fluid Power Transmission and Control, Department of Mechanical Engineering, Zhejiang University, China. He holds one Japanese patent in wearable sensors for gait analysis, which was commercialized. His current research interests include wearable sensor systems, rehabilitation robots, biomechanics, and human motion analysis. Dr. Liu was a recipient of the Japan Society of Mechanical Engineers Encouragement Prize in 2010. He received the Chinese Recruitment Program of Global Youth Experts in 2013.

Jingang Yi (S'99–M'02–SM'07) received the B.S. degree in electrical engineering from Zhejiang University, Hangzhou, China, in 1993, the M.Eng. degree in precision instruments from Tsinghua University, Beijing, China, in 1996, and the M.A. degree in mathematics and the Ph.D. degree in mechanical engineering from the University of California, Berkeley, in 2001 and 2002, respectively. He is currently an Associate Professor of Mechanical Engineering with Rutgers University. His research interests include autonomous robotic systems, dynamic systems and control, mechatronics, and automation science and engineering, with applications to biomedical systems and civil infrastructure and transportation systems.

Dr. Yi is a Fellow of the American Society of Mechanical Engineers (ASME). He was a recipient of the 2010 U.S. NSF CAREER Award. He has co-authored papers that have been awarded the Best Papers of the IEEE TRANSACTIONS ON AUTOMATION SCIENCE AND ENGINEERING, and at the IEEE/ASME AIM, ASME DSCC, IEEE ICRA, and so on. He currently serves as an Associate Editor for the IEEE/ASME TRANSACTIONS ON MECHATRONICS, the IEEE TRANSACTIONS ON AUTOMATION SCIENCE AND ENGINEERING, the IEEE ROBOTICS AND AUTOMATION LETTERS, the IFAC *Journals of Control Engineering Practice* and *Mechatronics*, the ASME *Journal of Dynamic Systems, Measurement and Control*, the *International Journal of Intelligent Robotics and Applications*, and the IEEE Robotics and Automation Society Conference Editorial Board since 2008. He also served as a Guest Editor for the IEEE TRANSACTIONS ON AUTOMATION SCIENCE AND ENGINEERING in 2009 and an Associate Editor for the ASME Dynamic Systems and Control Division Conference Editorial Board from 2008 to 2010.